

Kinetically Enhanced Fabrication of Homogeneous Biomimetic and Functional Emulsion Droplets

L. Pinon,^{†,‡,Ⓢ} L. Montel,[†] O. Mesdjian,[†] M. Bernard,^{†,§} A. Michel,^{||} C. Ménager,^{||} and J. Fattaccioli^{*,†,Ⓢ}

[†]PASTEUR, Département de Chimie, École Normale Supérieure, PSL University, Sorbonne Université, CNRS, 75005 Paris, France

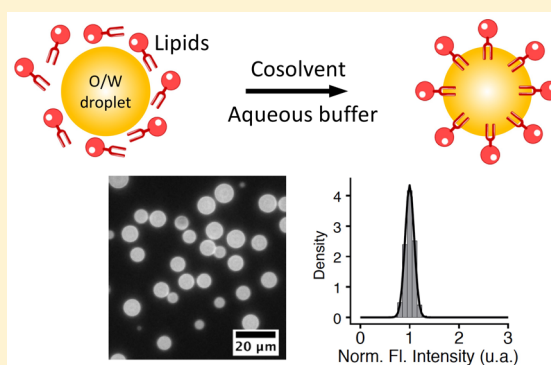
[‡]Institut Curie, PSL University, INSERM U932, 26 rue d'Ulm, 75248 Paris Cedex 05, France

[§]UMR 144, Institut Curie, 12 rue Lhomond, 75005 Paris, France

^{||}Sorbonne Université, CNRS, Laboratoire Physicochimie des Électrolytes et Nanosystèmes Interfaciaux PHENIX, 4 place Jussieu, F-75005 Paris, France

Supporting Information

ABSTRACT: Characterized by a fluid and deformable interface, ligand-functionalized emulsion droplets are used as model probes to address biophysical, biological, and developmental questions. Functionalization protocols usually rely on the use of headgroup-modified phospholipids that are dissolved in the oil phase prior to emulsification, leading to a broad range of surface densities within a given droplet population. With the aim to coat particles homogeneously with biologically relevant lipids and proteins (streptavidin, immunoglobulins, etc.), we developed a reliable surface decoration protocol based on the use of polar cosolvents to dissolve the lipids in the aqueous phase after the droplet production. We show that the surface density of the lipids at the interface has a narrow normal distribution for droplets having the same size. We performed titration isotherms for lipids and biologically relevant proteins on these drops. Then, we studied the influence of the presence of surfactants in the medium on lipid insertion and compared the results for a range of polar cosolvents of increasing polarity. To assess both the generality and the biocompatibility of the method, we show that we can produce more sophisticated, monodisperse functional magnetic emulsions with a very high surface homogeneity. Using an oil denser than the surrounding culture medium, we show that IgG-coated droplets can be used as probes for phagocytosis experiments.



■ INTRODUCTION

A wide range of liquid emulsified systems have been industrially developed over the past few decades with commercial applications in drug and oxygen delivery, in topical formulations, and dietary substitutes.¹ Utilizing their fluid and deformable interface, functional emulsion droplets were used recently as building blocks for liposome synthesis,^{2–4} biomimetic surfaces for cell adhesion modeling,^{5–7} cellular probes for phagocytosis⁸ and immune synapse studies,⁹ model particles for materials' self-assembly using DNA^{10,11} and adhesive protein binding,¹² and mechanical probes in the context of development¹³ and cell migration.¹⁴

Emulsion droplets can be fabricated with sizes spanning greater than 5 orders of magnitude, from a few tenths of nanometers to several hundred of microns. A high level of size uniformity is possible using methods such as membrane emulsification¹⁵ or microfluidic devices.¹⁶ In the literature, decoration of emulsion droplets with functional lipids, mostly phospholipids, is commonly achieved by dissolving the lipids in oil directly^{5,10,11} before fabricating the droplets using either: (1) a water-insoluble carrier solvent as chloroform^{8,17} to mix

the lipids with the oil prior to emulsification or by (2) dissolving the lipids in water in the presence of the droplets¹³ after their fabrication. Few studies were interested in measuring the homogeneity of the lipid insertion on the droplet surface at the level of the whole suspension. Those who showed that lipid insertion can vary significantly for droplets within the same production batch, no matter the technique used to fabricate the droplets, used protocols where lipids are dissolved in the hydrophobic phase prior to emulsification.¹⁸ The low solubility and tendency to form metastable aggregates such as liposomes¹⁹ for lipids dissolved directly in water are a major limitation in terms of functionalization efficiency. Hence, there is a need to develop reliable surface functionalization protocols able to overcome all of the aforementioned drawbacks.

As an alternative to previously published protocols, we modified the functionalization routines to improve the

Received: August 10, 2018

Revised: November 13, 2018

homogeneity and the kinetics of the surface lipid insertion among droplets of the same emulsion sample. Instead of dissolving the phospholipids in the oil prior to emulsification, we first fabricated the droplets and inserted the phospholipids at the droplet interface in a second step. We dissolved phospholipids in the aqueous continuous phase using a polar solvent, dimethyl sulfoxide (DMSO), that increases their availability and their insertion at the oil/water interface. The procedure leads to droplets with highly homogeneous surface lipid concentrations, characterized by a coefficient of variation (CV) as small as 10%. Using epifluorescence microscopy and flow cytometry as a means of characterization, we quantify both the kinetics and adsorption isotherms of lipids and proteins (IgG, streptavidin) specifically linked to biotin. Our experiments show that lipid insertion is optimal in the presence of a polar solvent, such as DMSO, in the continuous phase regardless of the variety. However, we show that the presence of surfactant micelles in the functionalization buffer is detrimental to the lipid insertion process. Finally, we show that the functionalization protocol can be used on more complex objects such as magnetic or halogenated oil droplets, and we show in the latter case that the emulsions can be used for phagocytosis experiments.

MATERIALS AND METHODS

Materials. Soybean oil (CAS no. 8001-22-7), mineral oil (CAS no. 8042-47-5), Pluronic F68 (CAS no. 9003-11-6), Tween 20 (CAS no. 9005-64-5), oleic acid (CAS no. 112-80-1), sodium alginate (CAS no. 9005-38-3), DMSO, acetonitrile, *N,N*-dimethyl formamide (DMF), pyridine, butanone, ethyl acetate, and triethylamine were purchased from Sigma-Aldrich (St. Quentin Fallavier, France). Lipiodol (CAS no. 8002-46-8) was a kind gift of the company Guerbet (Villepinte, France). DOPE-CF (1,2-dioleoyl-*sn*-glycero-3-phospho ethanolamine-*N*-(carboxyfluorescein)) and DSPE-PEG-biotin (1,2-distearoyl-*sn*-glycero-3-phospho ethanolamine-*N*-[biotinyl(polyethylene glycol)-2000]) were purchased from Avanti Polar Lipids. Alexa Fluor 488-conjugated mouse anti-biotin IgGs (ref. 200-542-211) were purchased from Jackson ImmunoResearch (Ely, U.K.). FluoProbes 488 streptavidin (ref. FP-BA2221) was purchased from Interchim (Montluçon, France).

Emulsion Fabrication with a Couette Emulsifier. Soybean oil or Lipiodol at a final oil fraction of 75 wt % is dispersed and emulsified by hand in an aqueous continuous phase containing 15 wt % Pluronic F68 block-copolymer surfactant [critical micellar concentration (CMC) = 0.03 g·L⁻¹²⁰ and 1 wt % sodium alginate. The rough emulsion is then sheared in a Couette cell apparatus²¹ to fabricate two quasi-monodisperse emulsion samples with average diameters of 5.5 ± 1.1 and 7.9 ± 1.7 μm. For storage and handling purposes, the emulsions are diluted to an oil fraction of 60 wt % with 1 wt % Pluronic F68 in the continuous phase and stored at 12 °C in a Peltier-cooled cabinet for several weeks.

Preparation of Phospholipid Stock Solutions in Polar Cosolvents. After evaporation of the phospholipid solvent (chloroform in our case), lipids are dissolved in a polar solvent at a concentration of 1 mg mL⁻¹ for DOPE-CF and 10 mg mL⁻¹ for DSPE-PEG-biotin. Stock solutions were prepared with DMSO, acetonitrile, DMF, pyridine, butanone, ethyl acetate, and trimethylamine.

Droplet Functionalization Protocol with Phospholipids. Emulsion droplets are diluted in a microtube at a concentration of 5 × 10⁶ droplets per μL in 200 μL of phosphate buffer (pH = 7.2 and 20 mM) supplemented with Tween 20 at a concentration corresponding to the CMC, i.e., 0.06 g·L⁻¹²². The suspension is centrifuged and rinsed four times with phosphate buffer (PB) to decrease the amount of Pluronic F68 in the continuous phase. After the last rinsing step, most of the continuous phase is removed from the microtube to decrease the total volume of emulsion to 10 μL. We

then add between 0 and 15 vol % of the polar stock solvent solution containing the phospholipids. We then add phosphate buffer with Tween 20 (CMC) to reach a total volume of 200 μL of suspension. Droplets are incubated for 90 min at room temperature in the presence of lipids in the bulk phase and rinsed several times with PB/Tween 20 CMC to remove the phospholipids in excess. The quantity of phospholipids available in the bulk phase at the initial stage is adjusted by diluting the stock solutions in their corresponding cosolvent so that the volume fraction of cosolvent remains constant for all experimental conditions. In most experiments, we use DMSO at a volume fraction of 10 vol %.

For a given working volume (200 μL), the lipid concentration in the bulk phase is expressed as a droplet surface area equivalent. One equivalent (equiv) of molecules corresponds to the number of molecules necessary to cover the total area of a population of droplets (5 × 10⁶ droplets, diameter = 8 μm) with a compact monolayer of molecules. The area per lipid is equal to 12.6 nm² for DSPE-PEG-biotin²³ and 0.5 nm² for DOPE-CF,²⁴ which corresponds to a volume of stock solution equal to 0.04 and 3.55 μL, respectively, to achieve 1 equiv of lipids in the working buffer.

Coating of Biotinylated Droplets with Antibiotin IgGs or Streptavidin. We add to the above solution (200 μL, 5 × 10⁶ droplets) a variable amount of stock solution of Alexa Fluor 488-conjugated mouse anti-biotin IgGs (0.8 mg mL⁻¹) or FluoProbes 488-conjugated streptavidins (1 mg mL⁻¹). After a 30 min incubation at room temperature in PB (pH = 7.2, 20 mM, Tween 20 at CMC), droplets are rinsed several times in the PB Tween 20 buffer to remove unreacted proteins. For 8 μm droplets, the volume of stock solution necessary to obtain a bulk concentration corresponding to 1 equiv of IgGs and streptavidin is, respectively, 2.5 and 5.78 μL. The molecular area we consider per IgG²⁵ and streptavidin²⁴ is, respectively, 120 and 16.6 nm². Size histograms and fluorescence intensity characterization results are reported in Figures S3 and S4.

Magnetic Emulsion Fabrication. The dispersed phase is composed of mineral oil, 10 vol % of the initial ferrofluid (γ-Fe₂O₃, 7 ± 1.6 nm, 1.57 M), and 5 vol % of oleic acid (see the Supporting Information for details about the ferrofluid synthesis). The continuous phase is an aqueous solution made of 15 wt % F68 in a phosphate buffer (pH = 7.2, 20 mM). Using a pressure regulator (MFCS, Fluigent, Paris), both the continuous and dispersed phases are injected into a microfluidic droplet generator. We obtain monodisperse droplets with an average diameter of 14.7 μm ± 2%. A representative bright-field microscopy image of the droplets and their size distribution are given in Figure S6B,C.

Analysis of the Adsorption Isotherms. Adsorption isotherms are fitted using a Langmuir adsorption model

$$\langle I \rangle = \langle I_0 \rangle \frac{KC}{1 + KC} \quad (1)$$

where $\langle I \rangle$ is the fluorescence density (see the Supporting Information for details), $\langle I_0 \rangle$ is the saturation value, C is the bulk concentration of lipids or proteins expressed in surface equivalents, and K is the apparent affinity constant.

Cell Culture and Handling. RAW 264.7 murine macrophages were purchased from ECACC. They were cultured in T-80 culture flasks (VWR) with Dulbecco's modified Eagle's medium (DMEM) 4.5 g/L L-glucose supplemented with 10% fetal bovine serum and 1% penicillin–streptomycin (Life Technologies), at 37 °C, and 5% CO₂. Twenty-four hours before experiment, they were detached using TrypLE (Life Technologies) and mechanical stimulation and seeded on 22 mm × 22 mm glass coverslips (VWR) in a 6-well culture plate (Corning) at 1 million cells per well.

Phagocytosis Experiments. The desired quantity of droplets (2 million per coverslip) is washed three times with a solution of Tween 20 (CMC) in a phosphate buffer. Droplets are then resuspended with anti-biotin Alexa 488 antibodies (Jackson ImmunoResearch) in PB/Tween 20 (CMC) solution, with antibodies in a 1:1 ratio compared to the DSPE-PEG2000-biotin available on the total surface of droplets. They are then incubated for 45 min at room temperature. The remaining antibodies are diluted at least 2000 times through 3

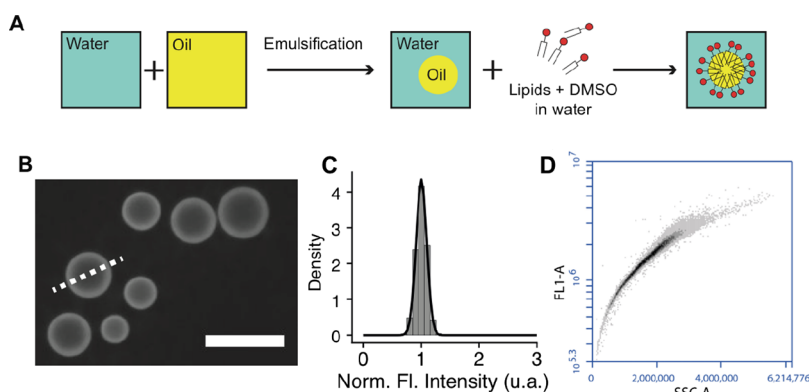


Figure 1. (A) Schematic representation of the functionalization routine used to coat emulsion droplets with phospholipids. Soybean oil is first emulsified and then phospholipids, which were dissolved using a polar cosolvent, are added to the bulk aqueous phase. The PCs migrate to the oil/water interface. When using functional phospholipids (e.g., biotinylated), antibodies or streptavidin can be conjugated to the droplet surface. (B) Representative image of DOPE-CF-functionalized droplets (2.5 equiv) recorded by spinning-disk confocal microscopy. Scale bar = 15 μm . (C) Fluorescence distribution of an emulsion subsample with a diameter of $7.9 \pm 0.5 \mu\text{m}$ (see Figure S1B for the size histogram). Experimental data are measured from wide-field epifluorescence microscopy and are fitted with a normal distribution (CV = 9%). Fluorescence intensities are normalized with respect to the average fluorescence value of the subset. (D) Density plot FL1 (fluorescence) vs SS (side scattering) obtained by flow cytometry in the case of IgG-coated droplets (100 equiv DSPE-PEG-biotin, 10 equiv IgGs) obtained following the protocol with a 10 vol % concentration of DMSO is used as a cosolvent to insert lipids into the interface after emulsification.

washing steps with PB/Tween 20 (CMC). PB/Tween 20 is then removed by a final centrifugation step (4000 rpm, 30 s for 8 μm large droplets), and droplets are finally diluted in 40 μL of culture medium (DMEM 4.5 g/L L-glucose w/o phenol red) at 37 $^{\circ}\text{C}$. Seeded glass coverslip is mounted on an open chamber formed by two coverslips separated by a 0.1 mm strip of double-sided tape, and then 2 million droplets suspended in DMEM are injected in the chamber. The droplets and cells are incubated together for 45 min at 37 $^{\circ}\text{C}$ 5% CO_2 ; then, the chamber is rinsed with phosphate-buffered saline. Cells are fixed in 4% paraformaldehyde solution.

Microscopy and Image Analysis. Bright-field and fluorescent images were acquired on a Zeiss Axio Observer Z1 microscope (Oberkochen, Germany) connected to a PCO Edge 4.2 sCMOS camera (PCO, Germany). Epi-illumination was achieved with a Lumencor Spectra X LED setup. Size distribution and fluorescence of the emulsion droplets were measured by microscopy and image analysis, respectively. All computations were performed with Fiji/ImageJ⁶ and R⁷ software. Droplets are observed with a Zeiss $\times 40$ objective (NA = 0.65). Spinning-disk microscopy recordings were performed using a Leica SD AF microscope with a $40\times$ objective. Images of the phagocytic assay were acquired using a Leica TCS SP8 laser scanning confocal microscope.

Flow Cytometry. Emulsion droplets were characterized with a BD Accuri C6 cytometer (BD Biosciences, New Jersey, USA).

RESULTS

We fabricate the droplets by manually shearing soybean oil, known to give stable and biocompatible emulsions,^{6,9,26,27} in an aqueous solution of a polymeric surfactant (Pluronic F68). We add a viscosifier to the continuous phase, sodium alginate, to increase its viscoelasticity and increase emulsification efficiency. The crude, polydisperse emulsion is then sheared in a Couette cell apparatus, following the method developed by Mason and Bibette.²¹ After emulsification and several rinsing steps of the continuous phase with an aqueous buffer containing Tween 20 at its CMC, we proceed to the lipid insertion onto the interface. Briefly, as summarized in Figure 1A, droplets are diluted in an aqueous buffer composed of amphiphilic functional lipids and a polar cosolvent, usually DMSO. Lipid insertion is assessed by fluorescence, using either microscopy or flow cytometry.

We first used a fluorescent phospholipid, DOPE-CF, dissolved in 10 vol % DMSO in water to study lipid insertion on the surface of $7.9 \pm 1.7 \mu\text{m}$ large soybean oil droplets (see Figure S1 for size distribution). Amongst all available polar cosolvents, DMSO is one of the most commonly used for cell biology experiments as a cryoprotectant in cellular systems,²⁸ membrane resealant,²⁹ or dilution helper. Figure 1B shows a representative spinning-disk confocal image of the droplets. Droplets have a homogeneous fluorescent interface and a near black center, as shown in Figures 1B and S2, indicating that fluorescent phospholipids are present only on the surface. Using a wide-field epifluorescence microscope, we measured the integrated fluorescence of the droplets over several thousand objects to assess their CV. Figure 1C shows the fluorescence distribution of a subsample of the original distribution having a diameter of $7.9 \pm 0.5 \mu\text{m}$ (see Figure S1B for the histogram). The fluorescence is highly homogeneous and follows a normal distribution with a CV of 9%.

We have demonstrated previously³⁰ that flow cytometry can be used to characterize emulsion droplets and, more specifically, their surface functionalization. Figure 1D shows the fluorescence versus side scattering intensity (SSC) density plot of IgG-coated droplets. Coating was achieved by insertion of DSPE-PEG-biotin molecules at the oil/water interface with the help of DMSO and further specific binding of antibiotin IgGs to the biotins (see Materials and Methods section for details). For a given SSC value, which roughly corresponds to a population of droplets with the same diameter,³⁰ the fluorescence range is very narrow, as expected from the fluorescence distribution shown in Figure 1C.

Interface and Affinity Characterization by Fluorescence Quantification. To measure and characterize the adsorption equilibrium of model fluorescent phospholipids on the emulsion interface, soybean oil droplets with a diameter of $7.9 \pm 1.7 \mu\text{m}$ are first functionalized using an aqueous solution containing 10 vol % of DMSO and a concentration of DOPE-CF lipids ranging from 0.1 to 20 equiv, expressed relative to a monolayer surface coverage as described in the Materials and Methods section. We quantify the amount of DOPE-CF lipids

by wide-field epifluorescence microscopy in an optical configuration that allows measuring the total amount of fluorescence present on the surface (see Figure S3 for details). Figure 2A shows a plot of the fluorescence density per droplet,

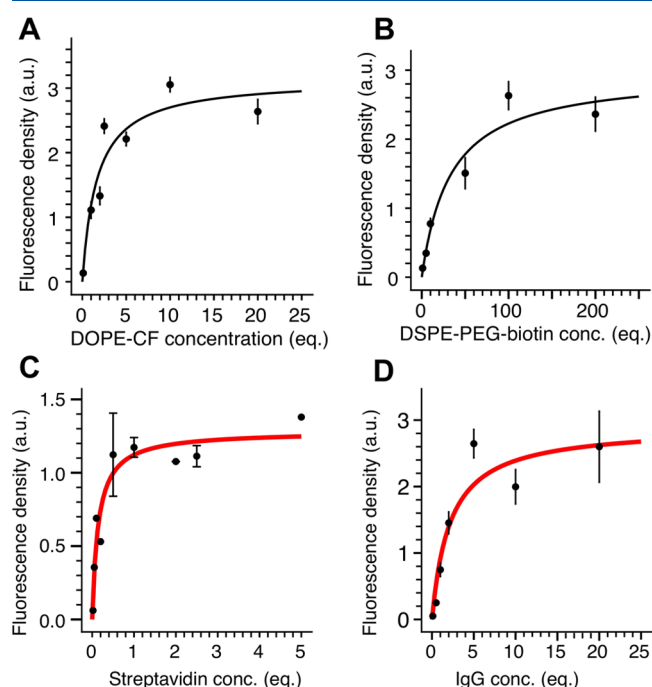


Figure 2. (A) Titration curve of droplets (average size: 8 μm) functionalized with DOPE-CF (10 vol % DMSO). Fluorescence density of the droplets is plotted as a function of the bulk concentration in DOPE-CF and expressed as a surface equivalent with respect to a monolayer. The titration curve is fitted by a Langmuir isotherm from which we extract an affinity constant between DOPE-CF and oil/water interface $K = 0.6 \pm 0.25 \text{ equiv}^{-1}$. (B) Titration curve of droplets functionalized with DSPE-PEG-biotin with respect to the biotinylated lipid bulk concentration. After insertion of the nonfluorescent biotinylated lipid, fluorescent IgGs are added to the bulk aqueous phase at a saturating concentration of 5 equiv. The curve follows a Langmuir isotherm with an apparent affinity constant $K = 0.03 \pm 0.015 \text{ equiv}^{-1}$. Titration curves for (C) streptavidin and (D) anti-IgG-coated biotinylated droplets, measured by epifluorescence microscopy. Soybean oil droplets are functionalized with 100 equiv of DSPE-PEG-biotin and an increasing bulk concentration of proteins. Titration curves are fitted by a Langmuir isotherm from which we extract an apparent affinity constant between proteins and oil/water interface equal to $K = 6.9 \pm 2.2 \text{ equiv}^{-1}$ and $K = 0.50 \pm 0.18 \text{ equiv}^{-1}$ for streptavidin and IgGs, respectively. NB: Maximal bulk concentrations were limited by the amount of available lipids and/or proteins.

defined as the ratio of the integrated fluorescence per object to its area (see the Supporting Information for details), as a function of the bulk concentration of DOPE-CF lipids. According to the fit, the affinity constant between DOPE-CF and the droplets is equal to $K_{\text{DOPE-CF}} = 0.6 \pm 0.25 \text{ equiv}^{-1}$.

We have shown in the past that emulsion droplets can be functionalized with biologically relevant proteins such as streptavidin^{6,9} or immunoglobulins (IgGs).⁸ DSPE-PEG-biotin molecules are inserted first at the oil/water interface and then are specifically bound to anti-IgGs or streptavidin. Here, we first dilute soybean oil droplets in a PB/Tween 20 CMC buffer containing 10 vol % DMSO and an initial DSPE-PEG-biotin concentration ranging from 0 to 200 equiv. After 90 min

of incubation at room temperature, we rinse the droplets according to the protocol reported in the Materials and Methods section. To reveal the presence of nonfluorescent DSPE-PEG-biotin and ultimately build the titration curve, we add a saturating amount fluorescent anti-IgGs (5 surface equivalents) to the suspension. After 30 min of incubation, we rinse the droplets and quantify their fluorescence by wide-field fluorescence microscopy. Figure 2B shows that the titration curve, plotted as the fluorescence density versus the bulk biotinylated lipid concentration, follows a Langmuir isotherm with an associated apparent equilibrium constant $K_{\text{DSPE-PEG-biotin}} = 0.03 \pm 0.015 \text{ equiv}^{-1}$. For DSPE-PEG-biotin, the binding constant is apparent because the titration is based on the quantification of anti-IgGs that bind to biotin but are much larger than the PEG-biotin moieties. The binding constant $K_{\text{DSPE-PEG-biotin}}$ should be interpreted as a binding capacity of the interface for IgGs rather than a molecular binding constant. It should ultimately depend on the surface DSPE-PEG-biotin concentration, although characterization of this parameter is beyond the scope of this study.

We measured the titration isotherms of the specific binding of streptavidin and anti-IgGs to the biotinylated droplets, knowing the apparent binding constant for the DSPE-PEG-biotin. First, droplets are biotinylated using a 10 vol % DMSO buffer solution containing 100 equiv of lipids, which is three times larger than the concentration corresponding to the biotinylated lipid binding constant measured previously. We then incubate the droplets for 30 min, which is much longer than the equilibrium time shown in Figure S5, in the solutions of streptavidin and IgGs with concentrations ranging, respectively, from 0 to 5 and 0 to 20 surface equivalents of proteins. The amount of protein on the surface saturates above 1 equiv of streptavidin and 10 equiv of IgGs, respectively, as shown in Figure 2C,D. Using a Langmuir adsorption model, we measure an apparent affinity constant of the proteins to the biotinylated droplets $K_{\text{streptavidin}} = 6.9 \pm 2.3 \text{ equiv}^{-1}$ and $K_{\text{IgG}} = 0.5 \pm 0.18 \text{ equiv}^{-1}$. These measurements are qualitatively in accordance with a larger affinity of streptavidin than anti-IgG for biotin^{31,32} in bulk condition, although absolute values cannot be easily extrapolated and compared in the context of our experiments.

Role of the Surfactant Concentration on Lipid Insertion. As detailed in the Materials and Methods section, droplet fabrication currently involves the use of two surfactants, Pluronic F68, used during the emulsification step and Tween 20, used during the functionalization step. Prior to functionalization, Pluronic F68 is usually rinsed out to reach a bulk concentration lower than its CMC. The presence of Tween 20 during the protein binding step is important not only to avoid droplet coalescence on the microtube walls but also to obtain a homogeneous coating of the droplets by dissociating small streptavidin and IgG aggregates. We have purposely selected surfactants that are used routinely in biological experiments^{33,34} to avoid possible biocompatibility issues related to their presence in the continuous phase.

To assess the influence of the surfactant type and concentration during a biotinylation step involving DSPE-PEG-biotin, we measured the mean fluorescence intensity of IgG-coated droplets as a function of these parameters. Table 1 shows the results obtained in the absence of any surfactant in the phospholipid solution and in the presence of Pluronic F68 or Tween 20 at concentrations equal and much larger than their respective CMCs during the biotinylation step. After

Table 1. Influence of the Surfactant Nature and Concentration Used during Biotinylation Step on the Fluorescence Distribution of the IgG-Coated Droplets (Diameter = $5.5 \pm 1.1 \mu\text{m}$)^a

sample	surfactant	Conc.	mean fluorescence (relative to sample #3)	SD	CV (%)
1	none		13.90	2.47	17.8
2	Pluronic F68	CMC	13.15	2.58	19.6
3	Pluronic F68	15 × CMC	1.00	0.09	9.1
4	Tween 20	CMC	14.81	2.48	16.8
5	Tween 20	10 × CMC	2.86	0.56	19.5

^aPluronic F68 and Tween 20 bulk concentrations are expressed with respect to their CMC. Sample 3 was chosen as a reference to ease the comparison of results.

incubation and rinsing, in all cases, the IgG binding step is performed in a PB/Tween 20 buffer at the CMC. Our measurements show that the presence of surfactants at high concentrations is detrimental to the insertion of lipids at the interface. At low surfactant concentrations, however, fluorescence intensities are maximized; they do not depend on the surfactant type and are similar to those measured in bare PB buffer. These results show that micelles compete with the droplet surface for lipid insertion and capture lipids that would have otherwise been able to migrate to the oil/water interface.³⁵ A confirmation of this could be obtained by measuring the fluorescence of the micelles in the bulk solution, where droplets are removed from the solution at the end of the procedure.

Role of the Cosolvent Nature and Concentration. To evaluate the influence of the nature of the cosolvent on the lipid binding to the droplets, we selected a number of common polar aprotic solvents to dilute the lipids prior to their insertion on the droplets. The solvents were ethyl acetate, pyridine, butanone, DMF, acetonitrile, triethylamine, and DMSO. All experiments were performed by diluting DOPE-CF or DSPE-PEG-biotin in pure cosolvents. The volume fraction is set to 10 vol % in the lipid insertion buffer. At the exception of triethylamine, whose presence quickly led to emulsion destabilization, all other cosolvents had no visible influence on droplet stability over the incubation time at room temperature. Lipid concentrations were chosen to be 2.5 equiv for DOPE-CF and 100 equiv for DSPE-PEG-biotin. Fluorescent anti-biotin IgGs were used at a 5 equiv concentration to reveal the presence of the biotinylated lipids. Figure 3 shows that for both lipids, the insertion is almost equivalent for all polar cosolvents, as the dependence upon their dipolar moment is very shallow.

When DMSO was used as a cosolvent, we quantified the effect of an increase of its volume fraction in the bulk phase by measuring the kinetics of lipid insertion for a DOPE-CF bulk concentration equal to 2.5 equiv. Figure 4A shows that the total fluorescence of DOPE-CF-coated droplets, measured by flow cytometry, increases with time and saturates at long-time scales for all experimental conditions. Kinetics is well described by a bounded first-order exponential equation. Figure 4B shows that larger DMSO concentrations allow a faster coating of the interface with a tenfold increase in the kinetics for a 15 vol % (0 to ca. 10 mol %) DMSO bulk concentration as compared to the case where no DMSO is present in the working buffer. Whereas the kinetic rate of lipid insertion at

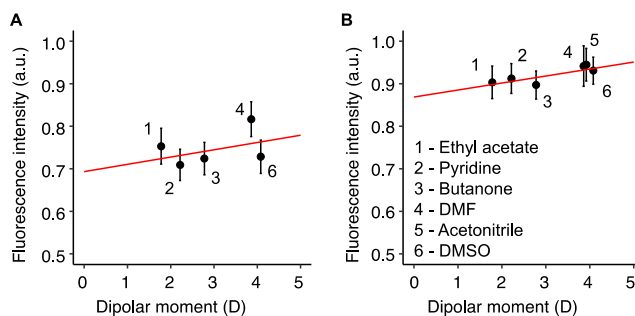


Figure 3. Total fluorescence intensity measured by flow cytometry of (A) 2.5 equiv DOPE-CF and (B) 100 equiv DSPE-PEG2000-biotin coated droplets in different nonpolar aprotic cosolvents during the lipid insertion step. The droplet diameter is $7.9 \pm 1.7 \mu\text{m}$, and IgGs were used at 5 equiv to reveal the presence of the biotinylated lipid. Lipids were diluted directly in the cosolvents, whose volume fraction has been set for all experiments to 10 vol %.

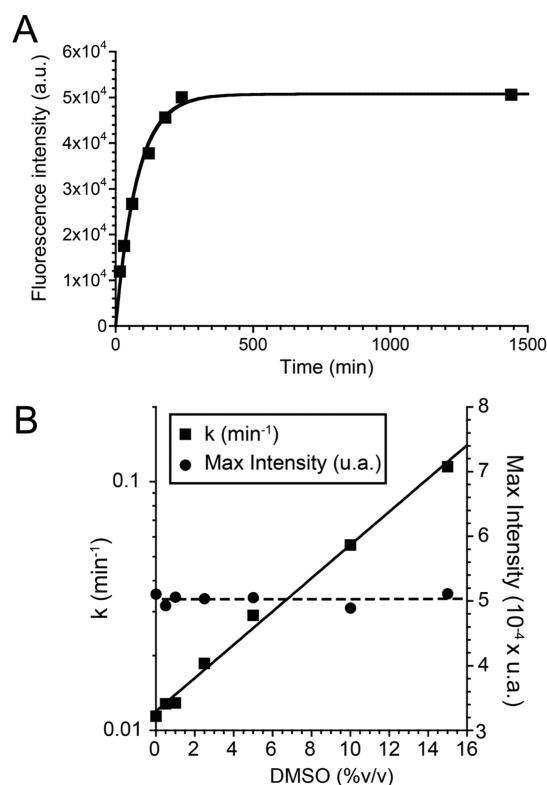


Figure 4. (A) Kinetics of the adsorption process onto the droplets measured by cytometry, for a DOPE-CF concentration of 2.5 equiv and a DMSO bulk concentration at 1 vol %. The integrated fluorescence of droplets has been measured by flow cytometry. Experimental data are fitted by an exponential function. (B) Reaction rate constant k (min^{-1}) of the adsorption process (■) and final fluorescence droplet intensity (●) plotted as a function of the DMSO bulk concentration ranging from 0 to 15 vol %. The reaction rate is fitted by a bounded exponential ($R^2 = 0.998$).

the oil/water interface scales exponentially with the DMSO bulk concentration, the final, thermodynamic value of droplet intensity does not depend on the DMSO concentration. These results indicate a kinetic enhancement of the lipid insertion process in the presence of the cosolvent instead of a thermodynamic effect.

Comparison to Previous Functionalization Methods. We formulate emulsion droplets following a commonly used

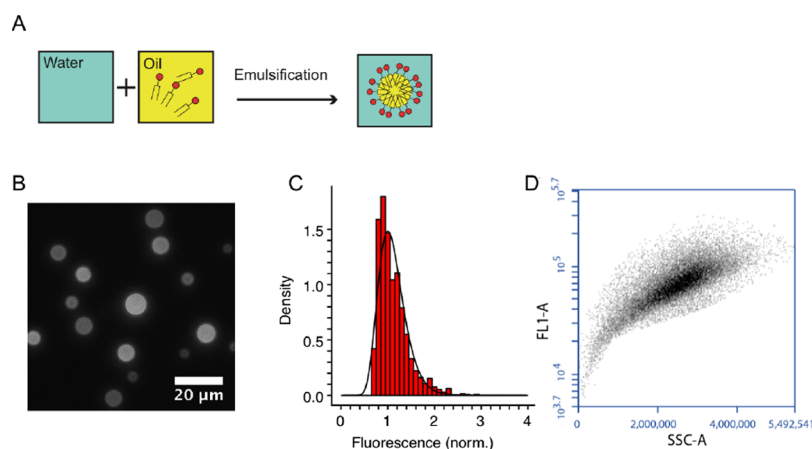


Figure 5. (A) Schematic representation of the previous functionalization protocol used to coat the emulsion droplets with phospholipids. Soybean oil containing functional phospholipids is directly emulsified. (B) Wide-field epifluorescence pictures of droplets ($7.8 \pm 1.9 \mu\text{m}$, see Figure S1C) functionalized with biotinylated phospholipids and further conjugated to fluorescent anti-biotin IgGs. Scale bar = $20 \mu\text{m}$. (C) Normalized fluorescence distribution of a droplet subsample (mean diameter: $7.9 \pm 0.5 \mu\text{m}$) coated with anti-biotin IgGs. Experimental data are fitted with a log-normal distribution ($\mu = -0.31$, $\sigma = 0.78$). Fluorescence intensities are normalized with respect to the average value of the whole population. (D) Density plots FL1 (fluorescence) vs SS obtained by flow cytometry in the case of IgG-coated droplets obtained following the protocol where lipids are diluted in the oil before emulsification.

protocol,⁸ in which biotinylated phospholipids are dissolved in the dispersed phase prior to emulsification (see Figure 5A). We first prepare a 10 mg mL^{-1} DSPE-PEG-biotin solution in chloroform, adding the stock solution to soybean oil to reach a final lipid concentration of 0.05 mg mL^{-1} . After evaporating the chloroform from the oil by moderate heating and sonication, we emulsify the oil, functionalize their interface with fluorescent anti-biotin IgGs, and finally quantify their fluorescence distribution. Figure 5B shows that the fluorescence of the droplets is not homogeneous amongst all of the droplets, which is confirmed both by the log-normal fluorescence distribution shown in Figure 5C and the cytometry density plot in Figure 5D. As compared to the fluorescence homogeneities of the droplets reported in Figure 1, the difference is striking with a clear advantage to the functionalization routine where lipids are brought to the oil/water interface from the continuous phase with the help of a polar cosolvent.

Validation of the Method and Biocompatibility. To demonstrate the broad applicability of the method developed in this work, we functionalized emulsion droplets characterized by a higher level of formulation complexity, made from a magnetic dispersed phase composed of a custom-made ferrofluid of $\gamma\text{-Fe}_2\text{O}_3$ nanoparticles suspended in mineral oil (see the Supporting Information for synthesis details). We then produced magnetic droplets using a pressure-controlled microfluidic flow-focusing device having channels with a rectangular cross section (Figure S6A). After emulsification, monodisperse droplets (Figure S6B,C) were functionalized with biotinylated phospholipids and fluorescent anti-biotin IgGs, for a DMSO concentration of 10 vol %. Fluorescence homogeneity across the sample is characterized by a CV equal to 10% as shown in Figure S6D. Upon application of a static magnetic field using a commercial permanent magnet, droplets align due to their superparamagnetic core (Figure 6A), which is the behavior we expect from such objects.³⁶

As a second example, to demonstrate the biocompatibility of the functionalization method, we performed a phagocytic assay of IgG-functionalized droplets, following an experimental procedure we developed recently.⁸ We first fabricated

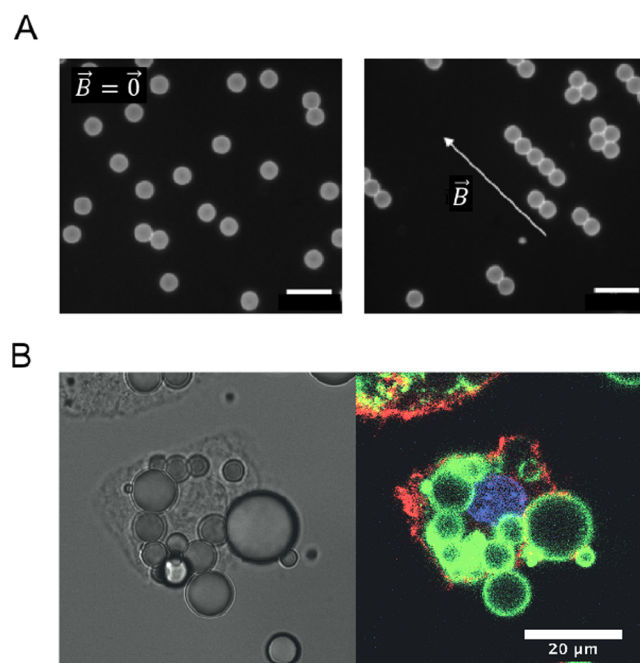


Figure 6. (A) Fluorescent images of monodispersed magnetic droplets (diameter = $14.7 \mu\text{m} \pm 2\%$) produced with a microfluidic flow-focusing device (see the Supporting Information for details). Droplets are biotinylated and further conjugated to fluorescent anti-biotin IgGs. In the absence of magnetic field (left), droplets are randomly distributed in the observation chamber, whereas when a magnetic field is applied (right), droplets align in its direction. Scale bar = $30 \mu\text{m}$. (B) Representative pictures of a phagocytic assay performed with IgG-coated droplets. RAW 264.7 macrophages are plated inside chambers, and droplets are suspended in the culture buffer and settle on the cells. After 45 min of experiment, the medium is rinsed and cells and droplets are fixed. After staining, bright-field (left) and fluorescence (right) pictures are recorded (red: F-actin, green: Alexa 488 anti-biotin IgG, blue: 4',6-diamidino-2-phenylindole/nucleus) and analyzed for quantitation. Scale bar = $20 \mu\text{m}$.

anti-biotin IgG-coated droplets from a pharmaceutical oil made from ethiodized fatty acid methyl ester (Lipiodol,

Guerbet); this oil has a high density ($d = 1.280$) and a sufficiently low viscosity allowing for easy emulsification. With such a formulation, functionalized droplets can be dispersed, rinsed, and finally used in a manner similar to common polystyrene beads, while having the additional feature of interfacial fluidity. Phagocytosis experiments are performed in an experimental chamber (see Figure S6A). Figure 6B shows that the presence of IgG on the droplets is a necessary condition (Figure S6B) to trigger a strong internalization by macrophages, in accordance with previous results.

DISCUSSION

Our results show that an increase of the DMSO concentration in the bulk phase enhances the kinetics of the lipid insertion at the interface without changing the lipid surface concentration at equilibrium. Phosphatidylethanolamine lipids have a negative curvature that favors their aggregation in the form of inverse hexagonal micelles. However, the presence of a carboxyfluorescein or a PEG biotin headgroup increases the overall lipid curvature to values compatible with lamellar self-assembly.³⁷ We hypothesize that functional phospholipids are present in the bulk phase as water-dispersed aggregates, such as direct micelles or liposomes, coexisting with a very small concentration of monomers.¹⁹ The fluorescence increase on the droplets over time is thus a consequence of a transfer of DOPE-CF lipids from the dissolved monomers and/or aggregates to the oil/water interface.

At the microscopic level, lipid transfer between two liposomes or between a liposome and another object such as an erythrocyte is possible through two different mechanisms that are experimentally difficult to discriminate.³⁸ Whereas in the first mechanism, lipid monomers dissociate from one bilayer, diffuse through the aqueous phase, and associate with the second membrane, the second mechanism involves lipid transfer during transient collisions between the objects.

The presence of DMSO in water has a strong influence on bulk properties such as the dielectric constant of the mixture that may alter the monomer/aggregate ratio and increase the concentration of free phospholipids in the bulk phase. This would result in an increase of the overall fluorescence of the droplets through the first lipid transfer mechanism described above. Experiments have been performed with a 2.5 equiv of DOPE-CF, which corresponds to a part of the adsorption isotherm that is very sensitive to the lipid concentration in the bulk aqueous phase (see Figure 2A). Increasing DMSO concentration could lead to different steady-state values of droplet fluorescence among samples, which is not the case, as shown in Figure 4B. This rules out the first mechanism as the main driving force of the fluorescence increase over time.

Subtle properties related to the phospholipids, such as the size of the hydration shell of their ionic headgroups or the repulsive force exerted by their lipid bilayer, depend on the concentration of DMSO and decrease for values corresponding to our experimental range.³⁹ In addition, oil droplets are stabilized by pegylated surfactants (Pluronic F68) that are characterized by a very long residence time at the interface.⁴⁰ With DMSO in the aqueous phase, Pluronic surfactants tend to become more hydrophobic⁴¹ as a consequence of the decreased range of the steric hydration force caused by dehydration of poly(ethylene oxide) groups.^{39,42} These arguments suggest that in the presence of a polar cosolvent in the aqueous phase, the short-range energetic barrier between the lipid aggregates and the droplets is lowered in a

concentration-dependent manner. As a consequence, the probability to have an effective lipid transfer in the event of a collision increases, hence explaining the kinetic enhancement shown by our quantitative results.

CONCLUSIONS

In this work, we developed and characterized a simple and reliable surface functionalization protocol allowing the fast and homogeneous insertion of functional lipids and ultimately biologically relevant proteins at the interface of oil-in-water emulsions. Lipids are brought to the interface from the aqueous phase with the help of a polar cosolvent, usually DMSO. We characterized the adsorption process and showed that the presence of micelles in the continuous phase was detrimental for functionalization. We showed that the adsorption is kinetically enhanced by the presence of the cosolvent and provide hypothesis that could explain the phenomenon. Finally, we have shown that the method is general and biocompatible. We applied it to the production of functional magnetic emulsions and to the production of IgG-coated emulsion probes for phagocytosis experiments.

ASSOCIATED CONTENT

Supporting Information

The Supporting Information is available free of charge on the ACS Publications website at DOI: 10.1021/acs.langmuir.8b02721.

Scaling relationship of the fluorescent intensity of the droplets with their size, ferrofluid synthesis protocol, microfluidic device protocol, size distribution histograms of the emulsion samples, representative spinning-disk confocal and wide-field fluorescence microscopy pictures of the emulsion droplets, fluorescence histograms of the droplets, kinetic fluorescence measurements of streptavidin and IgG adsorption on the droplets, bright-field image of the microfluidic flow focusing device used for the production of monodisperse magnetic droplets, and schematic view of the experimental setup used for phagocytosis experiments with droplets and comparative uptake histogram (PDF)

AUTHOR INFORMATION

Corresponding Author

*E-mail: jacques.fattaccioli@ens.fr.

ORCID

L. Pinon: 0000-0002-8645-071X

J. Fattaccioli: 0000-0002-0095-2576

Notes

The authors declare no competing financial interest.

ACKNOWLEDGMENTS

We thank Léa-Laetitia Pontani (Laboratoire Jean Perrin, Sorbonne Université) for fruitful discussions about the method, and Guerbet SA for having provided us Lipiodol samples. We are grateful to Andrew S. Utada (U. Tsukuba, Japan) for helping us to carefully edit the manuscript. This work has received support from the administrative and technological staff of "Institut Pierre-Gilles de Gennes" (Laboratoire d'excellence: ANR-10-LABX-31, "Investissements d'avenir": ANR-10-IDEX-0001-02 PSL and Equipement d'excellence: ANR-10-EQPX-34). L.P. acknowledges funding

from Sorbonne Université IPV Doctoral program. L.M. acknowledges funding from the Agence Nationale de la Recherche (ANR Jeune Chercheur PHAGODROP, ANR-15-CE18-0014-01).

REFERENCES

- (1) *Handbook of Pharmaceutical Excipients*, 6th ed.; Rowe, R., Sheskey, P., Quinn, M., Eds.; Pharmaceutical Press, 2009.
- (2) Pautot, S.; Frisken, B. J.; Weitz, D. A. Production of Unilamellar Vesicles Using an Inverted Emulsion. *Langmuir* **2003**, *19*, 2870–2879.
- (3) Matosevic, S.; Paegel, B. M. Stepwise Synthesis of Giant Unilamellar Vesicles on a Microfluidic Assembly Line. *J. Am. Chem. Soc.* **2011**, *133*, 2798–2800.
- (4) Abkarian, M.; Loiseau, E.; Massiera, G. Continuous Droplet Interface Crossing Encapsulation (CDICE) for High Throughput Monodisperse Vesicle Design. *Soft Matter* **2011**, *7*, 4610–4614.
- (5) Pontani, L.-L.; Jorjadze, I.; Viasnoff, V.; Brujic, J. Biomimetic Emulsions Reveal the Effect of Mechanical Forces on Cell-Cell Adhesion. *Proc. Natl. Acad. Sci. U.S.A.* **2012**, *109*, 9839–9844.
- (6) Fattaccioli, J.; Baudry, J.; Henry, N.; Brochard-Wyart, F.; Bibette, J. Specific Wetting Probed with Biomimetic Emulsion Droplets. *Soft Matter* **2008**, *4*, 2434–2440.
- (7) Bourouina, N.; Husson, J.; Waharte, F.; Pansu, R. B.; Henry, N. Formation of specific receptor-ligand bonds between liquid interfaces. *Soft Matter* **2011**, *7*, 9130.
- (8) Ben M'Barek, K.; Molino, D.; Quignard, S.; Plamont, M.-A.; Chen, Y.; Chavrier, P.; Fattaccioli, J. Phagocytosis of Immunoglobulin-Coated Emulsion Droplets. *Biomaterials* **2015**, *51*, 270–277.
- (9) Bourouina, N.; Husson, J.; Hivroz, C.; Henry, N. Biomimetic Droplets for Artificial Engagement of Living Cell Surface Receptors: The Specific Case of the T-Cell. *Langmuir* **2012**, *28*, 6106–6113.
- (10) Hadorn, M.; Boenzli, E.; Sorensen, K. T.; Fellermann, H.; Eggenberger Hotz, P.; Hanczyc, M. M. Specific and Reversible DNA-Directed Self-Assembly of Oil-in-Water Emulsion Droplets. *Proc. Natl. Acad. Sci. U.S.A.* **2012**, *109*, 20320–20325.
- (11) Feng, L.; Pontani, L.-L.; Dreyfus, R.; Chaikin, P.; Brujic, J. Specificity, flexibility and valence of DNA bonds guide emulsion architecture. *Soft Matter* **2013**, *9*, 9816.
- (12) Pontani, L.-L.; Jorjadze, I.; Brujic, J. Cis and Trans Cooperativity of E-Cadherin Mediates Adhesion in Biomimetic Lipid Droplets. *Biophys. J.* **2016**, *110*, 391–399.
- (13) Campàs, O.; Mammoto, T.; Hasso, S.; Sperling, R. A.; O'Connell, D.; Bischof, A. G.; Maas, R.; Weitz, D. A.; Mahadevan, L.; Ingber, D. E. Quantifying Cell-Generated Mechanical Forces within Living Embryonic Tissues. *Nat. Methods* **2013**, *11*, 183–189.
- (14) Molino, D.; Quignard, S.; Gruget, C.; Pincet, F.; Chen, Y.; Piel, M.; Fattaccioli, J. On-Chip Quantitative Measurement of Mechanical Stresses During Cell Migration with Emulsion Droplets. *Sci. Rep.* **2016**, *6*, 29113.
- (15) Joscelyne, S. M.; Trägårdh, G. Membrane emulsification—a literature review. *J. Membr. Sci.* **2000**, *169*, 107–117.
- (16) Leman, M.; Abouakil, F.; Griffiths, A. D.; Tabeling, P. Droplet-Based Microfluidics at the Femtolitre Scale. *Lab Chip* **2015**, *15*, 753–765.
- (17) Thiam, A. R.; Bremond, N.; Bibette, J. From Stability to Permeability of Adhesive Emulsion Bilayers. *Langmuir* **2012**, *28*, 6291–6298.
- (18) Giles, R. *Novel Magnetic Particles for Bioassays*; Université Pierre et Marie Curie: Paris VI, 2015.
- (19) Cevc, G. *Phospholipids Handbook*; CRC Press, 1993.
- (20) Samith, V. D.; Miño, G.; Ramos-Moore, E.; Arancibia-Miranda, N. Effects of Pluronic F68 Micellization on the Viability of Neuronal Cells in Culture. *J. Appl. Polym. Sci.* **2013**, *130*, 2159–2164.
- (21) Mason, T. G.; Bibette, J. Emulsification in Viscoelastic Media. *Phys. Rev. Lett.* **1996**, *77*, 3481–3484.
- (22) Mittal, K. L. Determination of CMC of Polysorbate 20 in Aqueous Solution by Surface Tension Method. *J. Pharm. Sci.* **1972**, *61*, 1334–1335.
- (23) Efremova, N. V.; Bondurant, B.; O'Brien, D. F.; Leckband, D. E. Measurements of Interbilayer Forces and Protein Adsorption on Uncharged Lipid Bilayers Displaying Poly(ethylene glycol) Chains†. *Biochemistry* **2000**, *39*, 3441–3451.
- (24) Banks, D. S.; Fradin, C. Anomalous Diffusion of Proteins Due to Molecular Crowding. *Biophys. J.* **2005**, *89*, 2960–2971.
- (25) Werner, T. C.; Bunting, J. R.; Cathou, R. E. The Shape of Immunoglobulin G Molecules in Solution. *Proc. Natl. Acad. Sci. U.S.A.* **1972**, *69*, 795–799.
- (26) Chenevier, P.; Veyret, B.; Roux, D.; Henry-Toulmé, N. Interaction of Cationic Colloids at the Surface of J774 Cells: A Kinetic Analysis. *Biophys. J.* **2000**, *79*, 1298–1309.
- (27) Bottier, C.; Fattaccioli, J.; Tarhan, M. C.; Yokokawa, R.; Morin, F. O.; Kim, B.; Collard, D.; Fujita, H. Active Transport of Oil Droplets along Oriented Microtubules by Kinesin Molecular Motors. *Lab Chip* **2009**, *9*, 1694–1700.
- (28) Lovelock, J. E.; Bishop, M. W. H. Prevention of Freezing Damage to Living Cells by Dimethyl Sulphoxide. *Nature* **1959**, *183*, 1394–1395.
- (29) Shi, R.; Qiao, X.; Emerson, N.; Malcom, A. Dimethylsulfoxide Enhances CNS Neuronal Plasma Membrane Resealing after Injury in Low Temperature or Low Calcium. *J. Neurocytol.* **2002**, *30*, 829–839.
- (30) Fattaccioli, J.; Baudry, J.; Emerard, J.-D.; Bertrand, E.; Goubault, C.; Henry, N.; Bibette, J. Size and Fluorescence Measurements of Individual Droplets by Flow Cytometry. *Soft Matter* **2009**, *5*, 2232–2238.
- (31) Green, N. M. Thermodynamics of the Binding of Biotin and Some Analogues by Avidin. *Biochem. J.* **1966**, *101*, 774–780.
- (32) Jung, H.; Yang, T.; Lasagna, M. D.; Shi, J.; Reinhart, G. D.; Cremer, P. S. Impact of Hapten Presentation on Antibody Binding at Lipid Membrane Interfaces. *Biophys. J.* **2008**, *94*, 3094–3103.
- (33) Watanabe, T.; Kitabatake, N.; Doi, E. Protective Effects of Non-Ionic Surfactants against Denaturation of Rabbit Skeletal Myosin by Freezing and Thawing. *Agric. Biol. Chem.* **1988**, *52*, 2517–2523.
- (34) Maskarinec, S. A.; Hannig, J.; Lee, R. C.; Lee, K. Y. C. Direct Observation of Poloxamer 188 Insertion into Lipid Monolayers. *Biophys. J.* **2002**, *82*, 1453–1459.
- (35) Stuart, M. C. A.; Boekema, E. J. Two Distinct Mechanisms of Vesicle-to-Micelle and Micelle-to-Vesicle Transition Are Mediated by the Packing Parameter of Phospholipid-Detergent Systems. *Biochim. Biophys. Acta, Biomembr.* **2007**, *1768*, 2681–2689.
- (36) Mandal, S. K.; Lequeux, N.; Rotenberg, B.; Tramier, M.; Fattaccioli, J.; Bibette, J.; Dubertret, B. Encapsulation of Magnetic and Fluorescent Nanoparticles in Emulsion Droplets. *Langmuir* **2005**, *21*, 4175–4179.
- (37) Hamai, C.; Yang, T.; Kataoka, S.; Cremer, P. S.; Musser, S. M. Effect of Average Phospholipid Curvature on Supported Bilayer Formation on Glass by Vesicle Fusion. *Biophys. J.* **2006**, *90*, 1241–1248.
- (38) Ferrell, J. E.; Lee, K. J.; Huestis, W. H. Lipid Transfer between Phosphatidylcholine Vesicles and Human Erythrocytes: Exponential Decrease in Rate with Increasing Acyl Chain Length. *Biochemistry* **1985**, *24*, 2857–2864.
- (39) Schrader, A. M.; Donaldson, S. H.; Song, J.; Cheng, C.-Y.; Lee, D. W.; Han, S.; Israelachvili, J. N. Correlating steric hydration forces with water dynamics through surface force and diffusion NMR measurements in a lipid-DMSO-H₂O system. *Proc. Natl. Acad. Sci. U.S.A.* **2015**, *112*, 10708–10713.
- (40) Pérez-Mosqueda, L. M.; Maldonado-Valderrama, J.; Ramírez, P.; Cabrerizo-Vílchez, M. A.; Muñoz, J. Interfacial Characterization of Pluronic PE9400 at Biocompatible (Air-Water and Limonene-Water) Interfaces. *Colloids Surf., B* **2013**, *111*, 171–178.
- (41) Ur-Rehman, T.; Tavelin, S.; Gröbner, G. Effect of DMSO on Micellization, Gelation and Drug Release Profile of Poloxamer 407. *Int. J. Pharm.* **2010**, *394*, 92–98.
- (42) Claesson, P. M.; Kjellander, R.; Stenius, P.; Christenson, H. K. Direct Measurement of Temperature-Dependent Interactions between Non-Ionic Surfactant Layers. *J. Chem. Soc., Faraday Trans. 1* **1986**, *82*, 2735.